

Maturation of the Electroretinogram
of the Neonatal Rabbit

John Gorfinkel, M.D.,
Department of Experimental Surgery
McGill University, Montreal

September 1987

A thesis submitted to the Faculty of Graduate
Studies and Research in partial fulfillment of the
requirements for the degree of Master of Science

© John Gorfinkel, M.D., 1987

Permission has been granted to the National Library of Canada to microfilm this thesis and to lend or sell copies of the film.

The author (copyright owner) has reserved other publication rights, and neither the thesis nor extensive extracts from it may be printed or otherwise reproduced without his/her written permission.

L'autorisation a été accordée à la Bibliothèque nationale du Canada de microfilmer cette thèse et de prêter ou de vendre des exemplaires du film.

L'auteur (titulaire du droit d'auteur) se réserve les autres droits de publication; ni la thèse ni de longs extraits de celle-ci ne doivent être imprimés ou autrement reproduits sans son autorisation écrite.

ISBN 0-315-46018-0

Table of Contents

1.1	Abstract	p. 3
1.2	Résumé	p. 4
2	Preface	p. 6
3	Introduction	p. 7
3.1	History	p. 7
3.2	Retinal histology	p. 8
3.3	ERG components	p. 10
3.31	ERP	p. 10
3.32	A-wave & B-wave	p. 13
3.33	C-wave	p. 14
3.34	Oscillatory potentials	p. 14
3.4	Purpose of study	p. 16
4	Methods	p. 17
4.1	Animal preparation	p. 17
4.2	Data collection & analysis	p. 19
5	Results	p. 25
5.1	Dark adaptation	p. 25
5.2	Light adaptation	p. 38
6	Discussion	p. 46
6.1	Dark adaptation	p. 46
6.2	Light adaptation	p. 49
7	Conclusions	p. 51
8	Acknowledgements	p. 53
9	References	p. 54
10	Appendix (tables of data)	p. 62

Abstract

The ontogenesis of the electroretinogram (ERG) in the rabbit has been stated to proceed first with the a-wave, then the b-wave and the oscillatory potentials (OPs) last. The significance of the OPs in the formation of the electroretinographic potential is a controversial issue. The aim of our study was to examine the role of the OP contribution to the ERG. Albino rabbits from the same litter were studied at weekly intervals for five weeks from the first week of life. A Grass photostimulator was used in light and dark adaptation and 50 amplified responses were averaged. Both 1-1000 Hz (ERG) and 100-1000 Hz (OP) bandwidths were recorded simultaneously. The a-wave was the first wave to appear at one to two weeks of age. The oscillatory potentials appeared sequentially as the rabbits aged. The change in waveform of the b-wave was consistent with the growth of each OP. The b-wave and oscillatory potentials evolved at the same rate, with an increase in amplitude and decrease in peak time. A rapid development was noted at two to three weeks, followed by a slower change. The simultaneous maturation of the b-wave and oscillatory potentials is contrary to previous reports and supports the contention that the OPs should be considered as major contributors to the b-wave.

Résumé

Des études antérieures ont démontré que l'ontogénèse de l'électrorétinogramme (ERG) chez le lapin débute d'abord par l'onde-a puis l'onde-b pour se terminer par l'apparition des potentiels oscillatoires (PO). Le but de notre étude fut d'examiner le rôle des potentiels oscillatoires dans la genèse de l'électrorétinogramme, ce sujet étant toujours fort controversé. Des lapereaux albinos, issus de la même portée, furent étudiés à intervalles réguliers pendant cinq semaines à compter de la première semaine de vie. Un stimulateur photique Grass a été utilisé en adaptation à la lumière ainsi qu'en adaptation à l'obscurité et cinquante réponses amplifiées furent moyennées. Deux bandes passantes furent utilisées simultanément: 1-1000 Hz (ERG) et 100-1000 Hz (PO). Les résultats démontrent que l'onde-a est la première à apparaître et ce pendant la deuxième semaine de vie, alors que les potentiels oscillatoires apparaissent de façon séquentielle au fur et à mesure que le lapin vieillit entraînant de ce fait des modifications à la morphologie de l'onde-b. L'onde-b et les potentiels oscillatoires mûrissent donc au même rythme où une augmentation dans les amplitudes s'accompagne d'un raccourcissement dans les temps de culmination. Ces modifications sont particulièrement accentuées entre la deuxième et troisième semaine de vie. Ces résultats suggèrent que les potentiels oscillatoires

doivent être considérés comme des constituants majeurs
de l'onde-b de l'électrorétinogramme.

Preface

The contribution to original knowledge in this paper relates to the oscillatory potentials (OPs), which are shown to be major contributors to the b-wave of the electroretinogram (ERG). This is in contrast to the view that the OPs are small appendages of the latter, and suggests that the OPs are important in analysis of the b-wave. Correlation between the development of the b-wave and oscillatory potentials is demonstrated in the growing rabbit. Many hitherto unexplained abnormalities of the ERG in retinal disease (specifically, the b-wave) may be explained by oscillatory potential changes. The oscillatory potentials are the key to future, more meaningful, ERG studies of retinal disease.



Introduction

History

The electroretinogram (ERG) was a mystery when Holmgren, in 1865, showed that an electrical potential (voltage) occurred between a corneal and optic nerve electrode in the frog eyeball, in response to a flash of light. Granit (1947) identified three components of the cat ERG that disappeared successively during deepening ether anaesthesia. He considered the ERG to be a summation of these processes, named P-I (c-wave), P-II (b-wave) and P-III (a-wave). The ERG came to be regarded as a massed response of the retina, the a-wave (initial negative wave) originating from the photoreceptors, followed by the b-wave (major positive wave) originating from the inner nuclear layer (Granit, 1962; Tomita, 1963; Brindley, 1957). The ERG became a valuable clinical tool for diagnosis of retinal disease when an extinguished ERG was found by Karpe (1945) to be an early sign of retinitis pigmentosa. Noninvasive experiments on the human eye became possible with the development of contact lens electrodes (Karpe, 1945; Henkes, 1951; Burian and Allen, 1954). This expanded the use of the ERG in studying human disease conditions. The complexity of the ERG was becoming apparent with the advance of electronic recording methods. Solutions to unwanted electrical noise in the signal involved the cumulation of analog output of the ERG amplifiers in

synchrony with a repetitive stimulus. Digital coding in the 1960's made possible computer averaging to do the same, by adding the response to repetitive stimuli and thereby cancelling out random noise. Microelectrode studies of the retina further revealed the intraretinal origins of the ERG (Tomita and Torihama, 1956; Brown and Wiesel, 1961).

Retinal histology

Vertebrate retinal architecture has been reviewed by Dowling (1970). The photoreceptors in the outer retina (outer nuclear layer) receive light and transmit the signal to the bipolar cells of the inner nuclear layer, which in turn provides input to the ganglion cells situated in the innermost retinal cell layer. Connections between the outer and inner nuclear layers are present in the outer plexiform layer, while the inner plexiform layer separates the inner nuclear and ganglion cell layers. The latter cells transmit the signal to the lateral geniculate bodies and then to the cortex. The Muller cells, with nuclei in the inner nuclear layer of the retina, are structural supporting cells of the retina. Almost all vertebrate retinas contain both rod and cone photoreceptors (Cohen, 1972), the former for low light vision and the latter for brighter colour vision. The rabbit retina contains rods, blue sensitive cones and green sensitive cones (Nuboer, van Nuys and Wortel, 1983) but is dominated by rods (Davis, 1929; Hughes, 1971).

The human retina contains rods, and cones sensitive to blue, green and red (Brown and Wald, 1964; Dartnall, Bowmaker and Mollon, 1983).

Gum et al. (1984) correlated the development of the ERG with the histological development of the retina in dogs. The appearance of the a-wave corresponded to the maturation of the photoreceptor layer from the outer neuroblastic layer at one week. The inner and outer plexiform layers were formed at the time of b-wave development during the third week, while further maturation of the inner nuclear layer correlated with an increase in amplitude and decrease in peak time of the b-wave. This would place the origin of the b-wave at the level of the inner nuclear layer.

ERG components

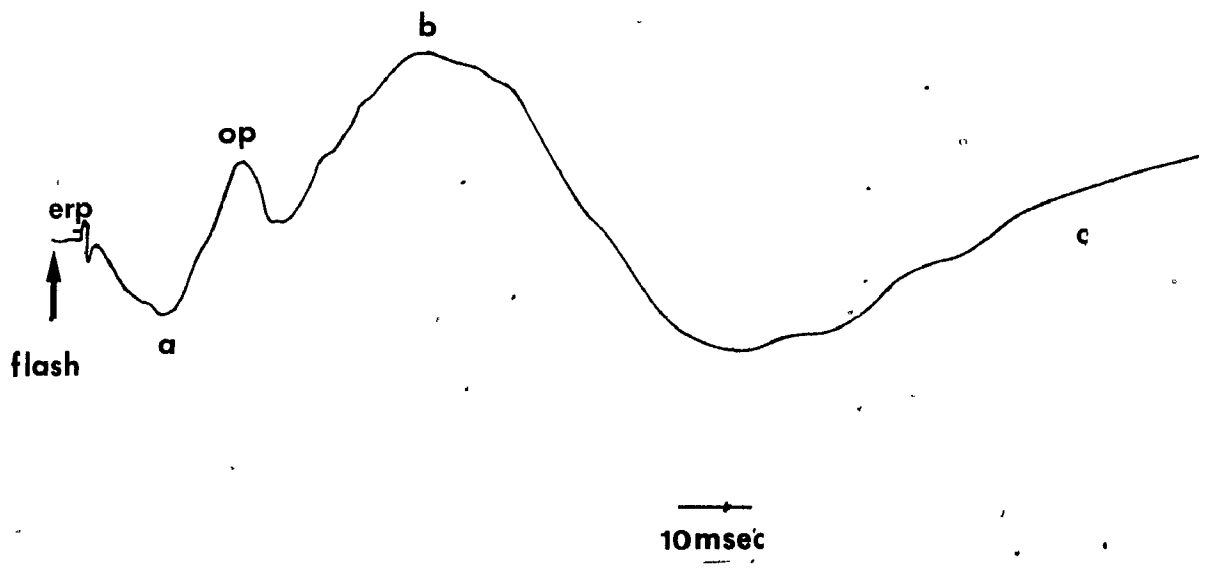
The ERG signal is broken down into successive waves, as shown in figure 1. These are correlated with the architecture of the retina, as described below.

Early receptor potential:

First in the ERG signal is the early receptor potential (ERP), a diphasic wave representing the photochemical changes and subsequent thermal reactions of molecules within the outer segments of cone receptors and, to a lesser extent, those of the rods (Brown and Murakami, 1964). It is the charge displacement in visual pigment units during conformational changes following light absorption that results in the ERP (Rodieck, 1973). The ERP is not generally seen in standard ERG recordings, because of a very short latency (<5 msec) and low voltage response (<1 μ volt) to light stimuli.

Figure 1: ERG components

A schematic ERG is shown. The individual waves that comprise the ERG are shown, as follows: the early receptor potential (ERP), the negative wave (a-wave), the most positive wave (b-wave), the oscillatory potentials (OPs), and the slow positive signal following the b-wave (c-wave). Vertical arrow indicates flash onset. Calibration: horizontal bar in milliseconds.



A-wave:

The a-wave is a corneal negative wave representing vertebrate photoreceptor hyperpolarization in response to a light (Tomita, 1970); that from cones appearing earlier than that from rods. A diminution of the dark current flowing from the photoreceptor inner segments to outer segments by a light stimulus causes this hyperpolarization (Penn and Hagins, 1972; Hagins et al., 1970).

B-wave:

The b-wave is the major positive wave of the ERG, originating from the Müller cells of the retina rather than from the bipolar cells, as thought earlier (Faber, 1969; Miller and Dowling, 1970). Components other than the Müller cells may contribute to the b-wave (Tomita, 1976). The bipolar cells take part in the processing of signals from the photoreceptors to the ganglion cells, while the Müller cells merely respond to the liberation of K⁺ ions by the bipolar cells (Miller and Dowling, 1970; Miller, 1973). Two different responses occur, depending on the state of light adaptation and stimulus intensity. A scotopic response is primarily rod mediated, elicited in dark adaptation in response to a dim light. It is of larger amplitude, longer duration and greater sensitivity to shorter wavelengths of light, compared to the photopic (light adapted, primarily cone) response.

C-wave:

The c-wave, a slow positive-going signal which follows the b-wave, is produced in large part by the hyperpolarization of the retinal pigment epithelium (Steinberg et al., 1970; Nilsson et al., 1977; Noell, 1954). It is seldom measured in clinical practise due to the contaminating muscle artefacts (Johnson and Massof, 1982).

Oscillatory potentials:

The oscillatory potentials (OPs) are ripples that appear on the ERG, formerly thought to be random variations. These have been considered as wavelets riding on the rising slope of the b-wave (Cobb and Morton, 1954). The maximum amplitude of intraretinal OP recordings has been noted in the inner nuclear layer of the frog retina, suggesting the latter to be the site of OP generation (Brindley, 1956). Ogden (1973) found the maximum intraretinal amplitude of the first three OPs to be at the level of the inner plexiform layer of the pigeon, chicken and monkey (Ogden, 1973; Ogden and Wylie, 1971). These layers have also been noted as the origin of the OPs by depth profile studies in the monkey (Heynen and van Norren, 1985). Both scotopic and photopic retinal systems produce oscillations independently of one another (Stodmeister, 1973; Fatechand, 1978).

Lachapelle et al. (1983, 1986a) have suggested that the OPs are building blocks of the b-wave. In

this view, the OP generated potentials could be integrated at the level of the Müller cells. They found that the ERG amplitude in congenital stationary night blindness (CSNB), in humans, was decreased in proportion to the absence of two OPs (Lachapelle et al, 1983). Others, however, have noted that the OPs are selectively abolished, as in diabetic retinopathy, suggesting separate processes for the b-wave and OPs (Yonemura et al., 1962; Brunette and Desrochers, 1970; Speros and Price, 1981).

Developmental analysis of the cat ERG by Hamasaki and Maguire (1985), where the formation of the a-wave preceded that of the b-wave and the appearance of the latter preceded that of the OPs, suggests a different origin for the b-wave and the OPs. In contrast, Sanada (1964a, 1964b) showed that the formation of OPs in suckling rabbits appeared as early as that of the a-wave wave. Noell (1958) studied ERG development in albino rabbits and noted that the a-wave developed first, at eight days of age, followed by the appearance of the b-wave at 10 days. The latter then developed rapidly to about 20 days. Similar results were also obtained from pigmented rabbits (Bonaventure et al., 1967). If the OPs are building blocks of the b-wave, one would expect them to develop simultaneously.

Study

The ERG is the only objective test available to assess retinal function. At present, only the peak time and amplitude of the b-wave are used in clinical diagnosis of retinal disease, yet there are numerous waveforms (including OPs) present in the ERG. In order to gain a better understanding of the generators of the ERG, I chose to study the development of the OPs and b-wave in the aging rabbit to determine if they mature at the same rate, and to analyse the contribution of the OPs to changes in b-wave morphology. We examined the ERG in light as well as dark adaptation. The animal model chosen reflects the clear illustration of the ERG by others in the frog, dog, cat, monkey, rabbit, and man (Brown, 1968). A better understanding of the generators of the ERG will permit more detailed clinical analysis of the ERG than is currently done, and should increase its diagnostic usefulness in disease.

Methods

Animal preparation

ERGs were recorded from six rabbits of the same litter. The mother and her litter were kept in the same cage on a 12 hour light:12 hour dark schedule in an ordinary animal room. The rabbits were anaesthetized with an intramuscular injection of ketamine (35 mg/kg) and xylazine (5 mg/kg). The earliest recordings were obtained at age seven days, on the day the eyes opened, and continued for five weeks. The rabbits were placed in a Faraday (shielded) chamber for recording, in order to remove electrical interference from the signal. The pupils were dilated with a drop of 0.5% tropicamide and 2.5% neosynephrine, and the cornea anaesthetized with a drop of 0.5% proparacaine. The ERGs were recorded with a speculum (Ag-AgCl) electrode which made contact with the upper and lower eyelids. Ag-AgCl was chosen for its low drift and low noise characteristics (Cooper, 1963; Strong, 1973; Jerris, 1974; Geddes, 1972). The speculum electrode also served to keep the eye open. A drop of 0.9% saline solution was placed in the cul-de-sac of the eye to promote electrical contact between the speculum and the eye. The left eye was used consistently.

The experimental setup is illustrated in figure 2 (p. 21). The reference and ground inputs were connected and a common electrode was placed in the

mouth of the rabbit. The rabbits were placed in a diffusing container, with a background illumination of 520 lux for studies in light adaptation, and were dark-adapted for 15 minutes for studies in dark adaptation. ERGs were evoked to flashes of white light with a Grass PS-22 photostimulator (Grass Instrument Company, Quincy, Massachusetts). The flash was set at an intensity of $10.0 \text{ cd/m}^2/\text{sec}$, delivered at a rate of one flash/sec, for light adapted studies, and at 0.3 and $3.2 \text{ cd/m}^2/\text{sec}$, delivered at a rate of one flash/5 sec, for dark adapted studies.

ERGs were recorded simultaneously with two Grass P-511 AC preamplifiers. One amplifier had a bandwidth of 1-1000 Hz and an amplification factor of 2000 X to record the usual a-b wave ERGs. The other amplifier had a bandwidth of 100-1000 Hz (and an amplification of 20,000 X), suggested for selective recording of the OP₃ of the ERG (Dawson and Stewart, 1968; Kozak, 1971; Tsuchida et al., 1973; Wachtmeister and Dowling, 1978). An amplifier with a recording bandwidth of 30-1000 Hz (and an amplification of 10,000 times) was added at weeks 4 and 5. An average of 50 flashes was determined with the Nicolet MED-80 signal averager. This permitted the removal of electrical noise by spreading out the random positive and negative waves over time. The response of the eye to light, however, was selectively amplified, as the stimulus, recording onset and response were synchronized. Interstimulus

intervals of 1024 msec, in light adaptation, and 4096 msec, in dark adaptation, were generated by a Grass model S10VS interval generator. These time intervals were chosen so as not to be a multiple of 60, in order to further minimize the contribution of 60 Hz noise. The recordings were stored in digital form on floppy disks by the Nic-299 diskette storage unit. A hard copy of the response was obtained with a Hewlett Packard 7010B x-y plotter (Hewlett Packard Company, Palo Alto, California).

Data collection

In order to maximize the data collection and at the same time avoid repeated anaesthesia of the same rabbit, each rabbit was tested only once a week and always on the same day. Thus, for any given rabbit there was always a one week interval between consecutive measurements (longitudinal study). Furthermore, each rabbit served as a means to monitor the rate of maturation of the ERG occurring within one week (transverse study). A tattoo, on an ear or foot of each rabbit, permitted identification of each rabbit for data acquisition.

Data analysis

The nomenclature for naming ERG waves and OPs is shown in figure 3. The a-wave amplitude and peak time were measured from the baseline, at flash onset, to the trough of the a-wave. The ERG signal was dissected

into subcomponents, as follows: the amplitudes of the individual positive waves of the ERG (1-1000 Hz) recordings, numbered 2 to 5 (see note in figure 3), were measured from the trough of the a-wave to the peak of each wave (where the most positive peak is defined as the b-wave), while the peak times were measured from flash onset to each wave peak. The OP amplitudes on the OP (100-1000 Hz) recordings were measured from each trough to peak, and peak times were measured from flash onset to the individual peaks of the OPs.

Figure 2: Experimental setup.

A-Light from the photostimulator reached the rabbit through the diffusing barrier.

B-The rabbit was placed in the Faraday chamber and the recording electrode was placed under the lids of the left eye, while the ground and reference electrodes were placed in the mouth.

C-The computer recording and light source were synchronized with a timing device (flash onset 20 msec after computer sweep).

D-The signal was relayed to amplifiers with filtering bandwidths as in the text.

E-The computer performed an average of 50 responses to light, from the output of the amplifiers.

F-The output from the amplifiers was also channelled to the oscilloscope for monitoring.

G-Hard copies of the data were printed with a plotter.

H-The data were stored on floppy disks.

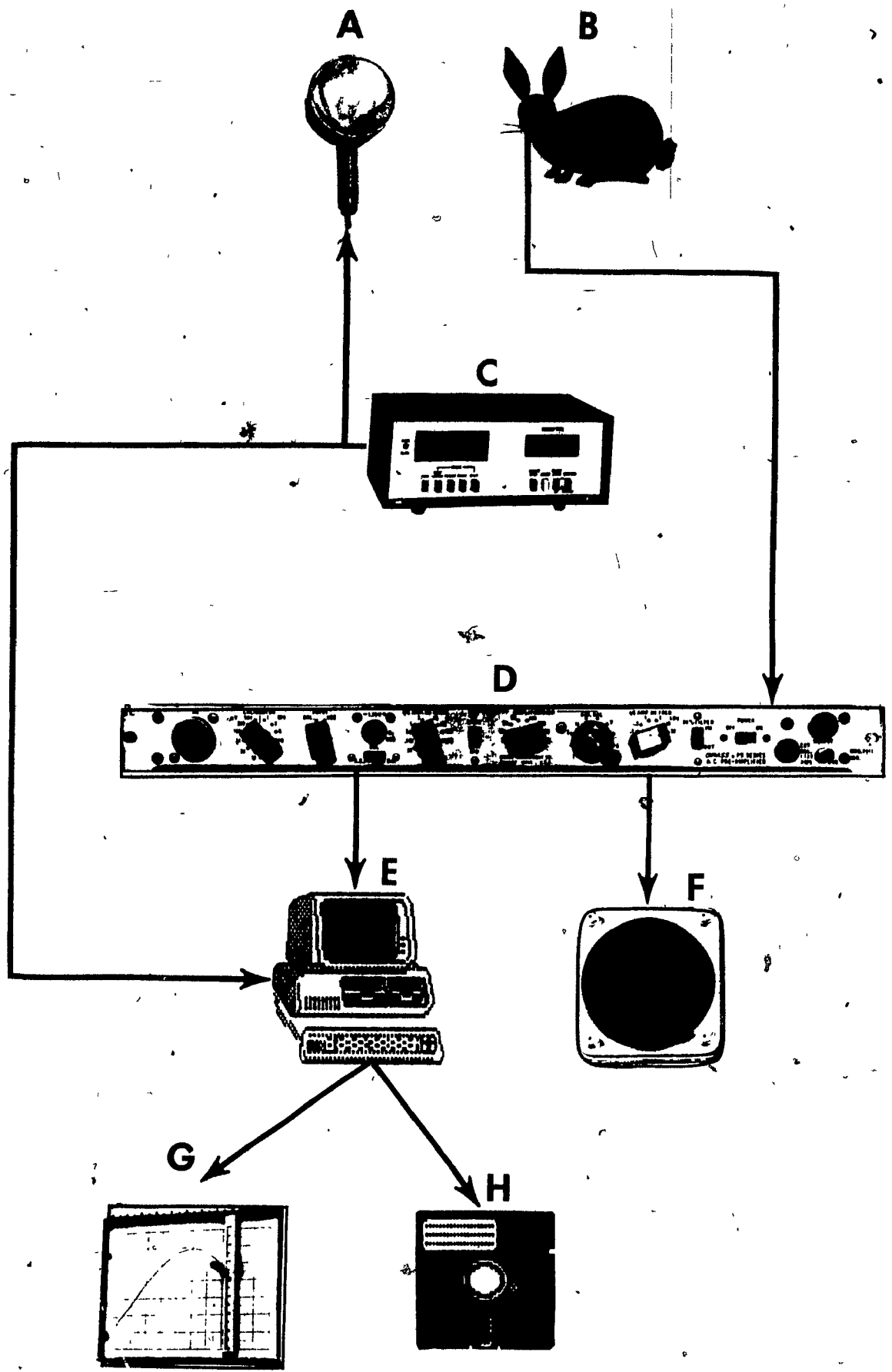
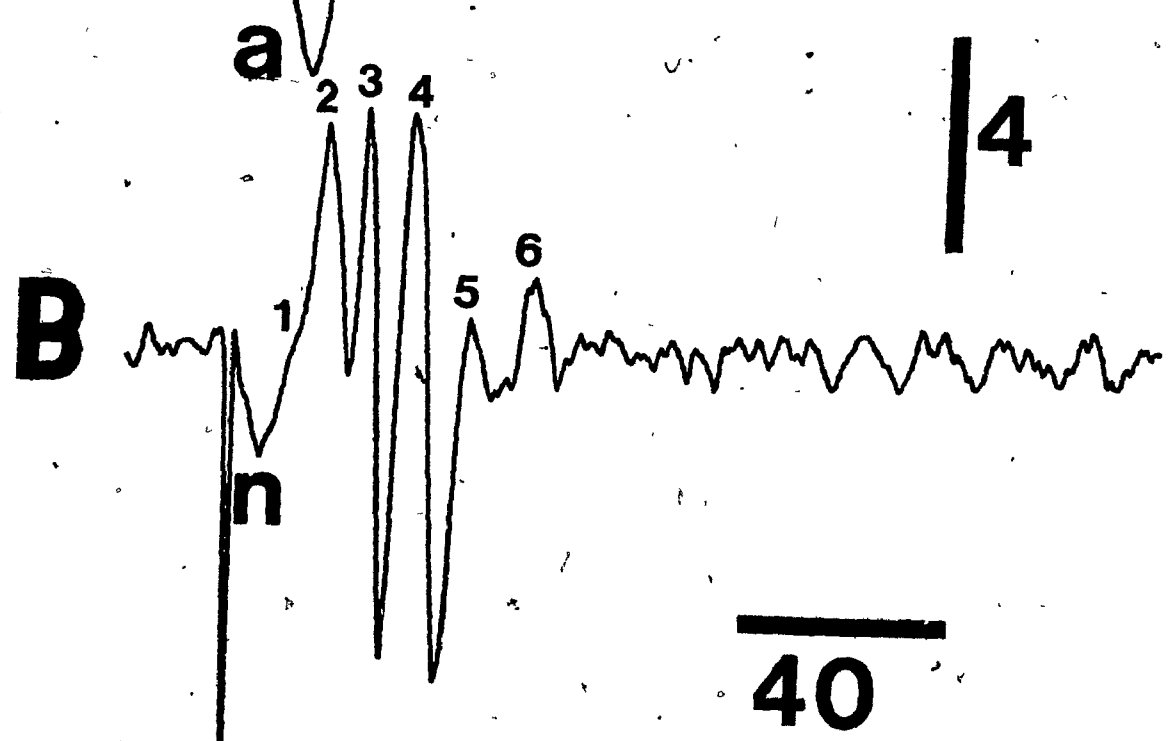
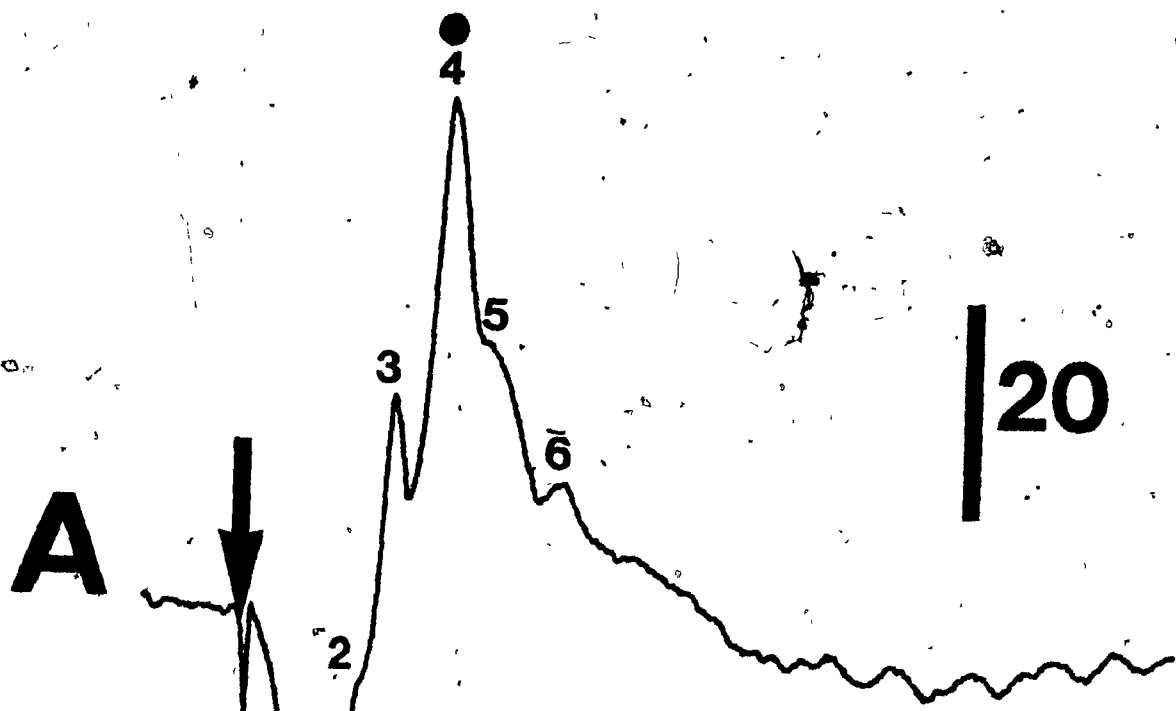


Figure 3: Recording procedures and wave analysis.

The ERG (1-1000Hz bandwidth :A) and the OPs (100-1000Hz:B) were recorded simultaneously with amplification factors of 2000X for the ERG and 20,000X for the OPs. The ERG positive waves are numbered according to the OP nomenclature, except for the negative wave which is labelled a-wave in the ERG recordings and n-wave in the OP recordings. OP 1 is small and not always seen on the OP recordings, and is not visible on the ERG recordings; thus the numbering of positive waves from 2 onwards. The wave corresponding to the peak of the b-wave (most positive portion of the ERG) is identified with a dot.

The vertical arrow indicates flash onset. Calibration: horizontal bar in milliseconds, vertical bar in microvolts.



Results

Dark Adaptation

The results for a flash intensity of $3.2 \text{ cd/m}^2/\text{sec}$ (bright flash) are shown in figure 4 and summarized in figure 5. The b-wave and corresponding OPs increase in amplitude and decrease in peak time with advancing age. A rapid progression in both the b-wave and OP recordings is seen between week 2 and week 3. From week 3, however, the OPs and b-waves increase in amplitude and decrease in peak time at a regular rate. The ratio of summed OP amplitude to b-wave amplitude (SOP/b-wave: figure 5) remains constant at 22% as the rabbit ages, suggesting that both increase at the same rate. The time interval between consecutive OPs (OP-OP: figure 5) decreases with age, indicating that the frequency domain of the OPs increases significantly ($t=4.98; df=8; p=.005$) from $97 \pm 10 \text{ Hz}$ at week 3 to $122 \pm 12 \text{ Hz}$ at week 5.

The b-wave and OPs can be seen to develop between day 7 and day 14 in the transverse study illustrated in figure 6. At day 7 the b-wave peaks at 42.3 msec, at day 8: 25.4 msec, at day 9: 75.4 msec, and at day 14: 53.8 msec. This variability is due to changing peak times and number of OPs, as the rabbits mature, that contribute to the b-wave (more OPs are present at day 9 vs. day 7). Some OPs (marked by arrows in figure 6) at days 7 and 8 are small and ill-defined, but can be better visualized if compared with those at days 9

Figure 4: The effect of aging on the dark-adapted ERG and OPs (flash intensity $3.2 \text{ cd/m}^2/\text{sec}$) weekly measurements: two rabbits illustrated.

ERG recordings of two rabbits are shown in A and C, with corresponding OP recordings in B and D, respectively. The vertical arrow indicates flash onset. Calibration: horizontal bar in milliseconds, vertical bar in microvolts.

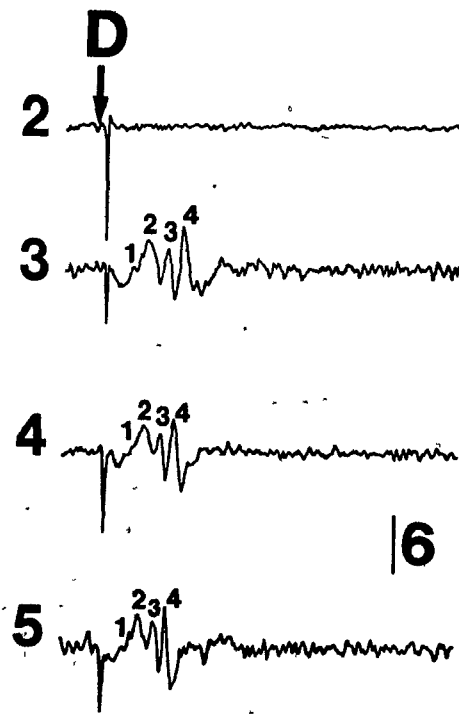
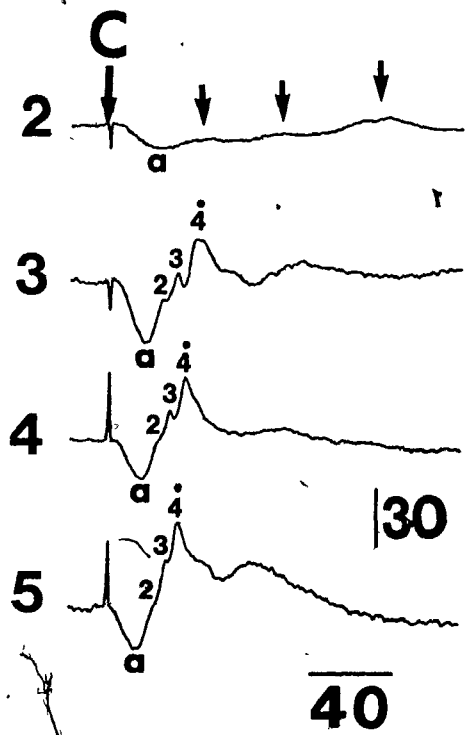
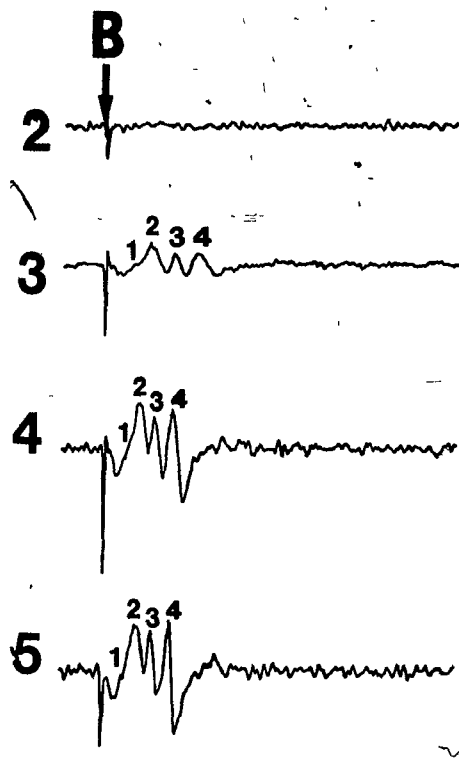
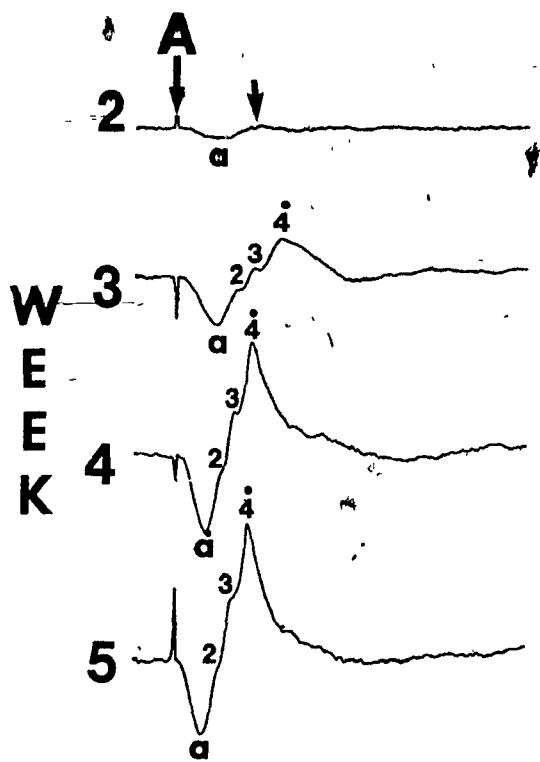


Figure 5: Summary of ERG and OP measurements with age
(flash intensity 3.2 cd/m²/sec) weekly data.

a-amp (a-wave amplitude), a-pt (a-wave peak time), b-amp (b-wave amplitude), b-pt (b-wave peak time), SOP (summed amplitudes OP2,3,4), OP-pt (OP peak time), OP/b % (ratio of SOP to b-wave amplitude in percent), OP-OP' (inter OP time interval). Data points represent mean \pm 1 standard deviation. Amplitudes are measured in microvolts, time in milliseconds.

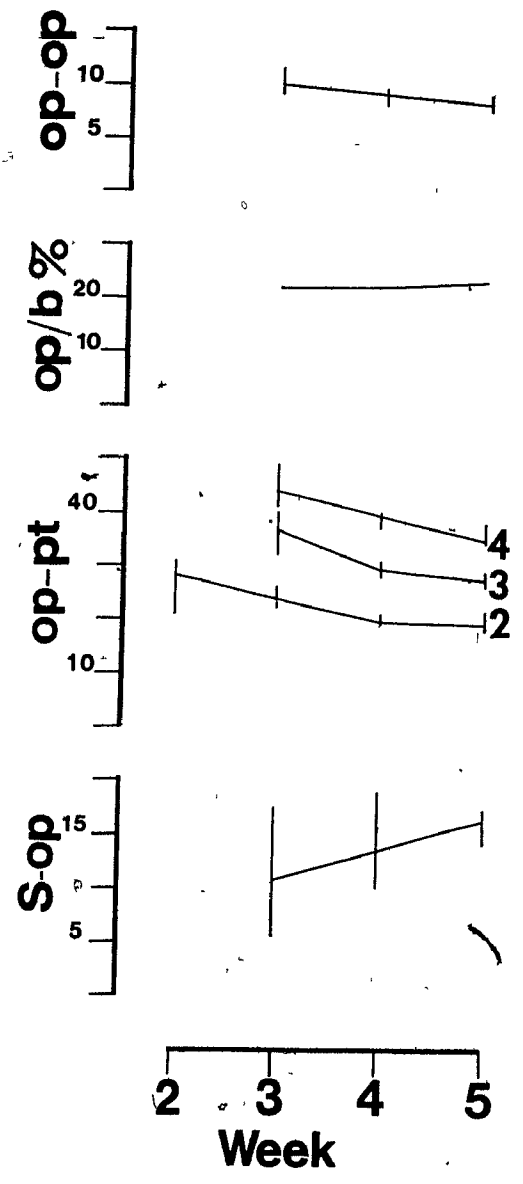
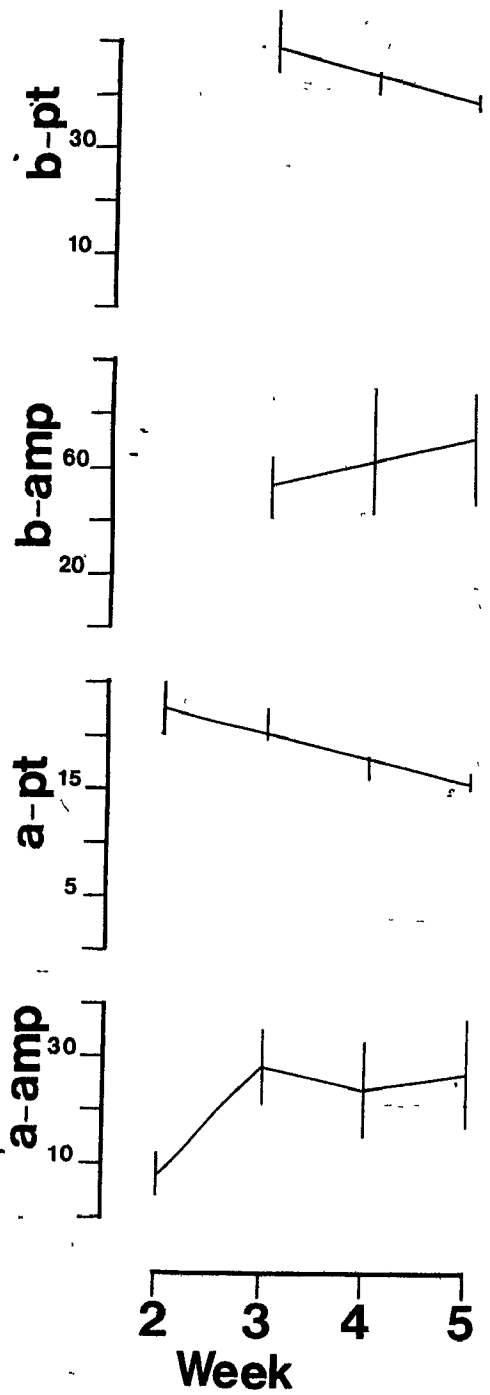
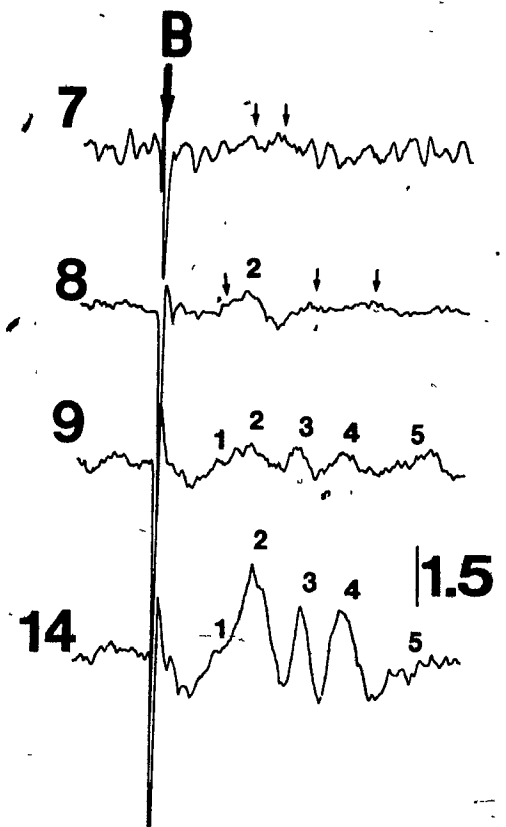
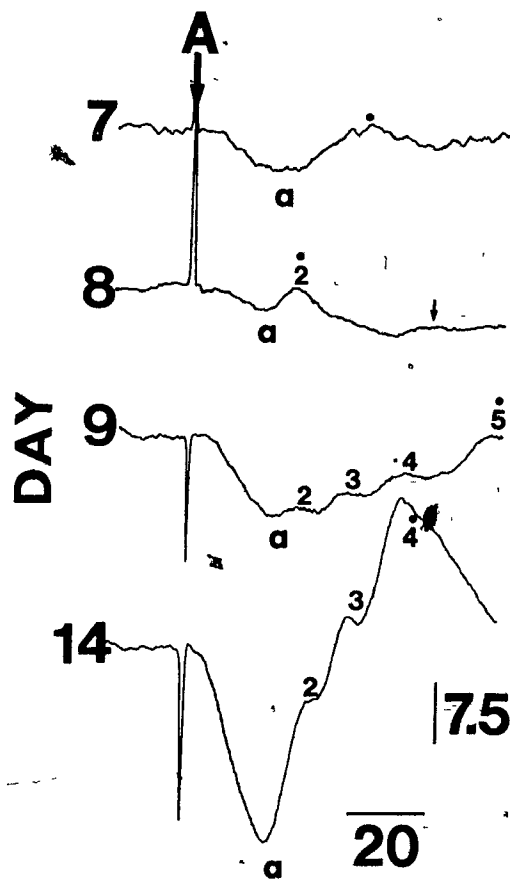


Figure 6: The effect of aging on the dark-adapted ERG and OPs (flash intensity 3.2 cd/m²/sec) daily measurements: transverse study.

ERG recordings are shown in A, with corresponding OP recordings in B. The small arrows indicate poorly visible OPs that are better appreciated by comparison with larger OPs of similar peak time at later days. The vertical arrow indicates flash onset. Calibration: horizontal bar in milliseconds, vertical bar in microvolts.



and 14. At days 7 and 8, OP2 forms the b-wave while at day 9, the OP recording shows well delimited OP2, OP3, OP4 and OP5. The latter is now responsible for the peak of the b-wave. The rapid increase in the amplitude of the a-wave added to the low voltage of the OPs, seen at day 9, fails to produce a b-wave of mature morphology. Rather, the ascending limb of the "b-wave" looks more like a slow drift towards a baseline value. The typical b-wave is achieved between day 9 and day 14, when the OPs have reached an amplitude large enough to counteract the electronegativity produced by the a-wave. At day 9, all OPs (OP2,3,4,5) have similar amplitudes and can be seen to contribute equally to the rising phase of the b-wave. At day 14, however, OP2,3,4 are significantly larger than OP5 and thus become the major b-wave contributors.

The recordings done with a flash intensity of $0.3 \text{ cd/m}^2/\text{sec}$ (dim flash) are shown in figure 7. With advancing age, the amplitude of the b-wave increases and the peak time decreases. The OPs (figures 7B, 7D) are not visible until the fifth week. Recordings in figure 8B, done at four weeks of age, show minimal OPs with the 100-1000 Hz bandwidth (see arrows), but show the presence of OP-like waves that are clearly visible with a 30-1000 Hz bandwidth recording. A similar effect is noted in figure 8A at five weeks of age. The frequency domain of the OPs is 90 Hz at week 5, a

frequency not affected by a 30-1000 Hz bandwidth, but one attenuated to noise levels by a 100-1000 Hz bandwidth. These results suggest that the OP recordings in figure 7 could be flat because of attenuation by a bandwidth, where the low frequency cut-off is too high for the frequency domain of the OPs being recorded.

Figure 7: The effect of aging on the dark-adapted ERG
(flash intensity 0.3 cd/m²/sec).

ERG (A,C) and OPs (B,D) simultaneously recorded from two rabbits. The tilted arrows mark discontinuities on the slope of the b-wave, which represent OPs. The vertical arrow indicates flash onset. Calibration: horizontal bar in milliseconds, vertical bar in microvolts.

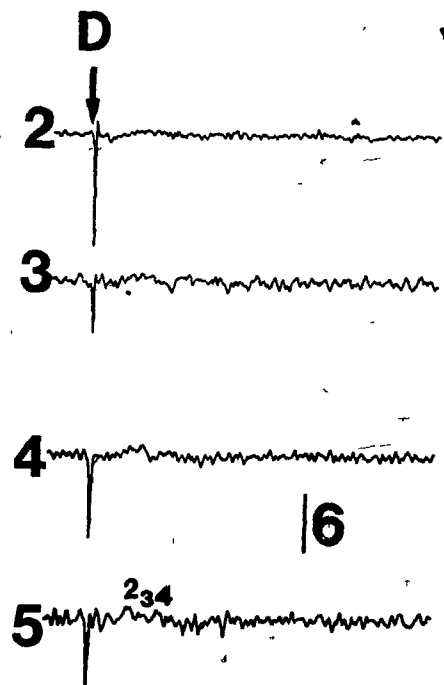
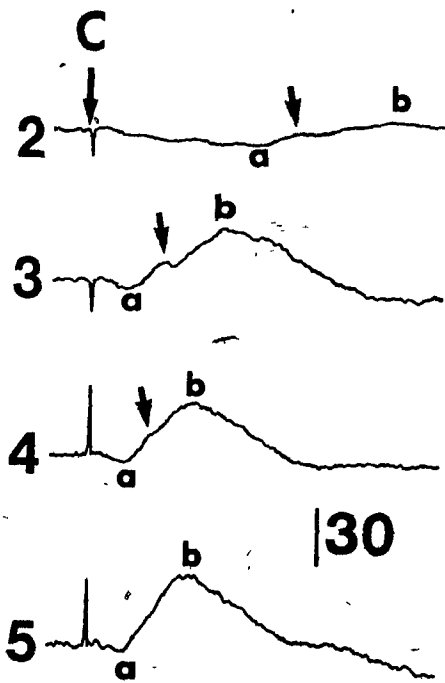
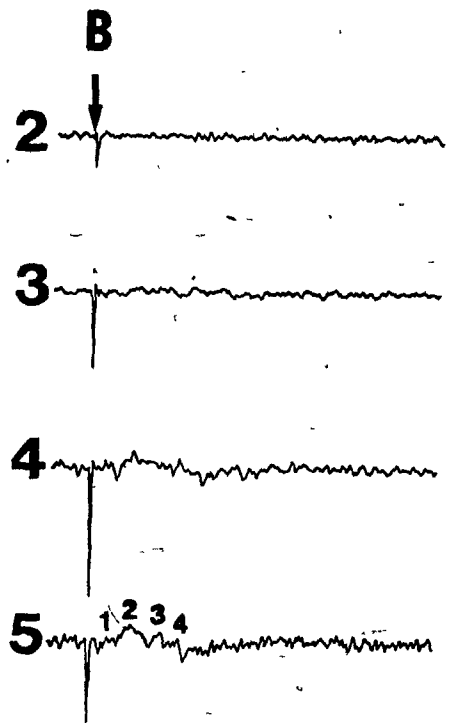
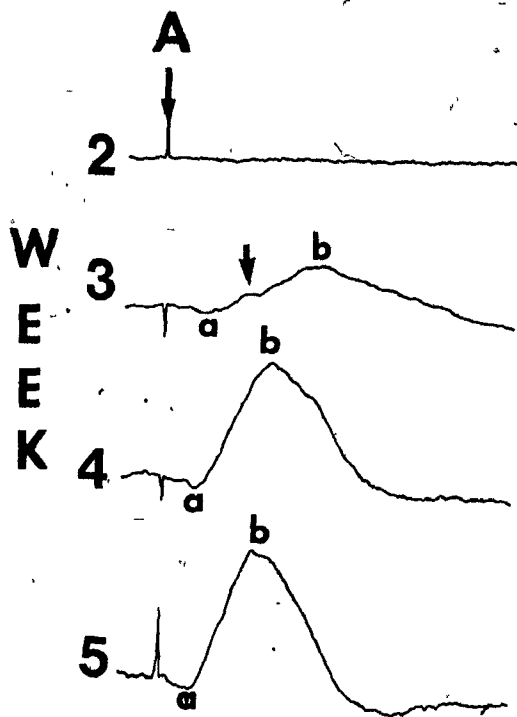
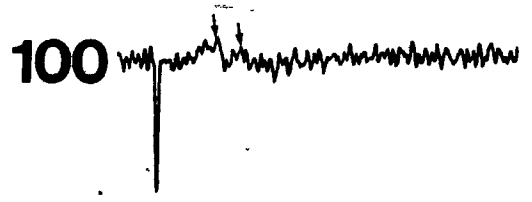
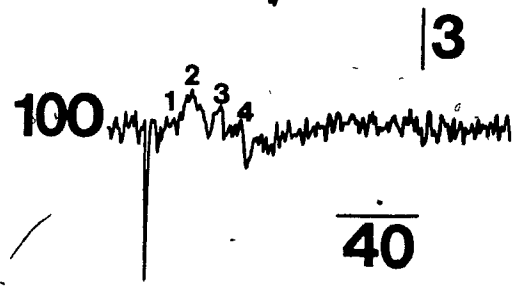
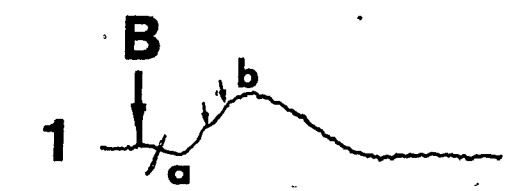
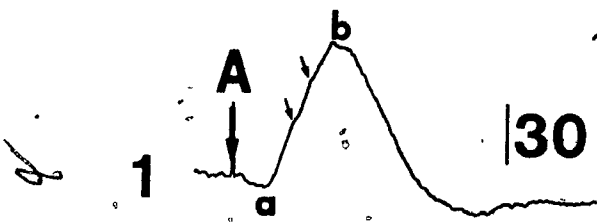


Figure 8: Modification of the ERG signal produced by different bandwidths.

Dark-adapted (intensity: $0.3 \text{ cd/m}^2/\text{sec}$: tracings A,B) recorded from two different rabbits. All three recording bandwidths 1-1000Hz, 30-1000Hz and 100-1000Hz, as shown on the left hand side of each tracing, were recorded simultaneously. The 30-1000Hz recording was amplified 10,000X. The third tracing is almost flat, while the 30-1000Hz recording demonstrates "OP like" waves (figure B). Tilted arrows point to discontinuities in the first tracing and small OPs in the third tracing that correspond in time to the OP-like waves seen in the 30-1000 Hz recording. The vertical arrow indicates flash onset. Calibration: horizontal bar in milliseconds, vertical bar in microvolts.



Light Adaptation

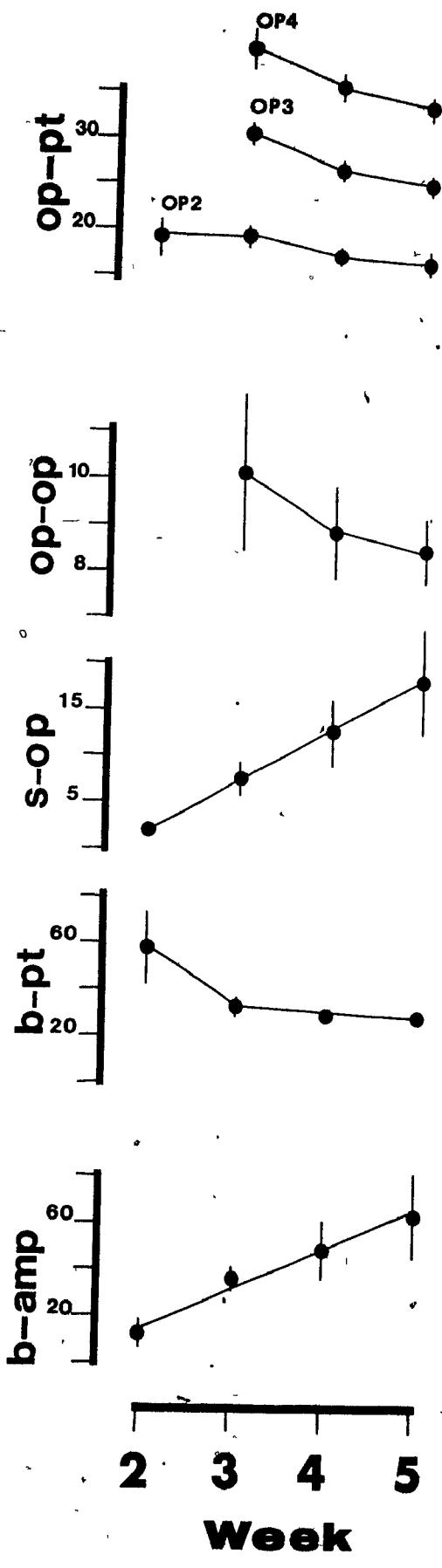
The b-wave amplitude increases at a regular rate with age, while the peak time decreases (figure 9). Likewise, the summed amplitude of the OPs increases and the peak time of the individual OPs decreases, as the rabbits mature. The interpeak interval of the OPs can be seen to decrease from 10.1 ± 1.7 msec at week 3 to 8.4 ± 0.7 msec at week 5, which represents an increase in frequency domain of the OPs from 99 ± 16 Hz to 119 ± 10 Hz. A set of recordings, typical of the majority of rabbits, is shown in figure 10A, where the b-wave (which always corresponds to the peak of wave 3) increases in amplitude and decreases in peak time, with age. The other individual positive waves (waves 2 and 4) change similarly, with an increase in amplitude and decrease in peak time. However, in the recordings in figure 10C, a different picture emerges, where the b-wave peak time corresponds to wave 3 at both the third and fourth weeks, but shifts to wave 4 at the fifth week (the b-wave by definition being the most positive wave). This results in an increase in peak time of the b-wave at the fifth week. The development of the ERG is similar in figures 10A and 10C, the difference being the wave peak number corresponding to the peak of the b-wave in the fifth week. The OPs on the OP (100-1000 Hz) recordings (figure 10D) can be seen to develop sequentially and each corresponds, in peak time, to the individual positive waves on the ERG

(1-1000 Hz) recordings.

The importance of the OPs in determining the amplitude and peak time of the b-wave is further illustrated in figure 11; the recording at week 4 shows an ambiguous situation where two equally positive peaks are present, both measuring 62.7 microvolts from the trough of the a-wave. If one considers wave 4 as the b-wave, wave 3 would be an OP. However, should wave 3 be considered the b-wave by virtue of ontogenesis (since wave 3 is the highest peak at an earlier week), wave 4 would have to be considered as an OP occurring after the peak of the b-wave.

Figure 9: Summary of ERG and OP measurements with age
(background intensity 520 lux, flash intensity 10.0
cd/m²/sec) weekly data

b⁻amp (b-wave amplitude), b-pt (b-wave peak time), SOP
(summed amplitudes OP_{2,3,4}), OP-pt (OP peak time), OP-
OP (inter OP time interval). Data points represent
mean ± 1 standard deviation. Amplitudes are measured
in microvolts, time in milliseconds.



A

Figure 10: Maturation of the light-adapted ERG:
weekly measurements (background: 520 lux; flash
intensity: 10 cd/m²/sec)

There was more variability of measurements dealing with the b-wave in light versus dark adaptation. Wave 4 takes over wave 3 in amplitude at week 5 (figure C) causing a sudden shift in b-wave peak time. The presence and amplitude of the individual OPs correspond to the individual waves, similarly numbered, on the ERG. However, the highest peak is always the same (wave 3) in figure A. The highest peak is also always the same (wave 4) in dark adaptation, from week 3 onwards (figure 4), resulting in a regular change of b-wave parameters with age. The vertical arrow indicates flash onset. Calibration: horizontal bar in milliseconds, vertical bar in microvolts.

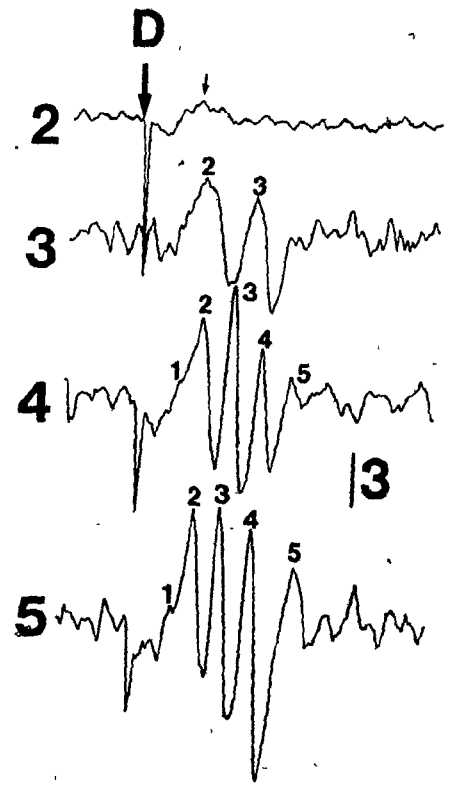
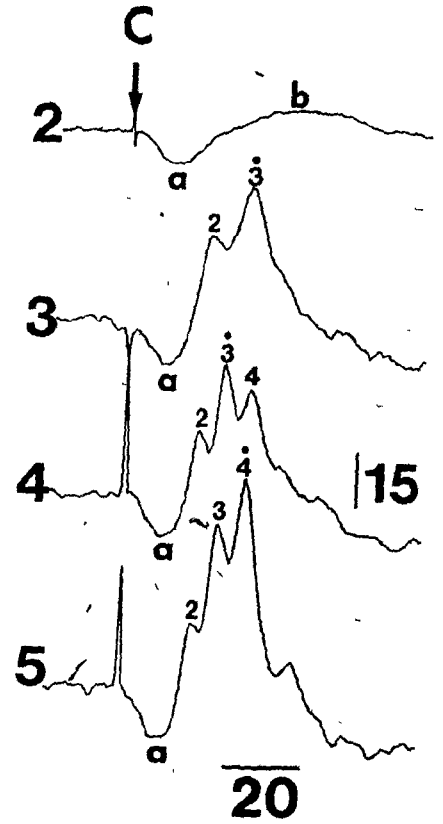
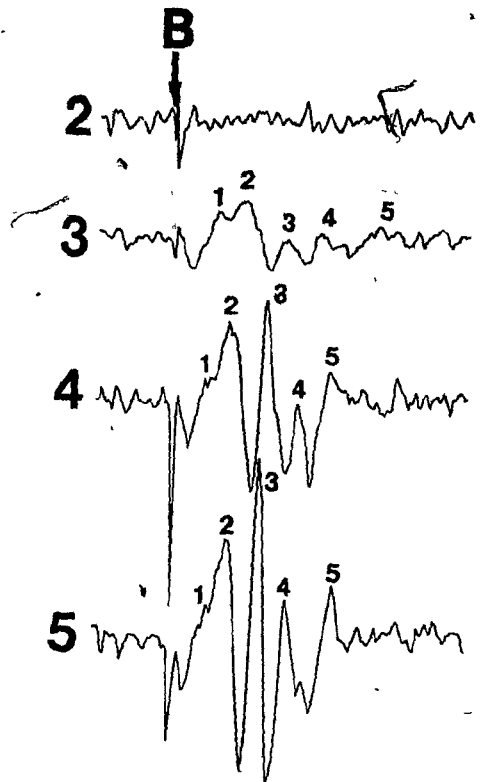
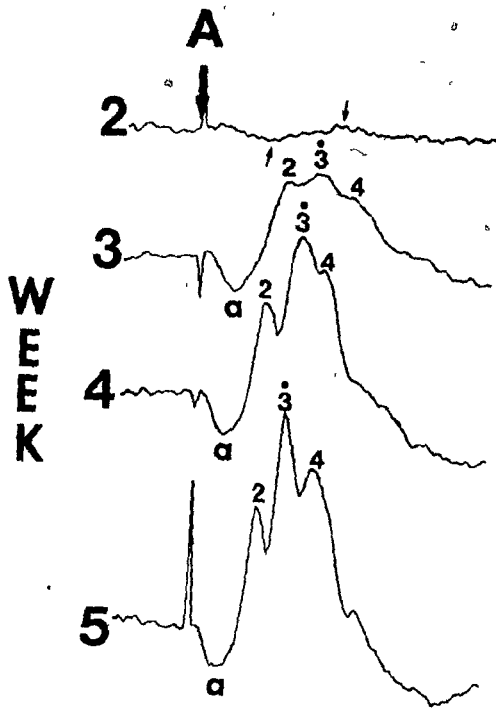
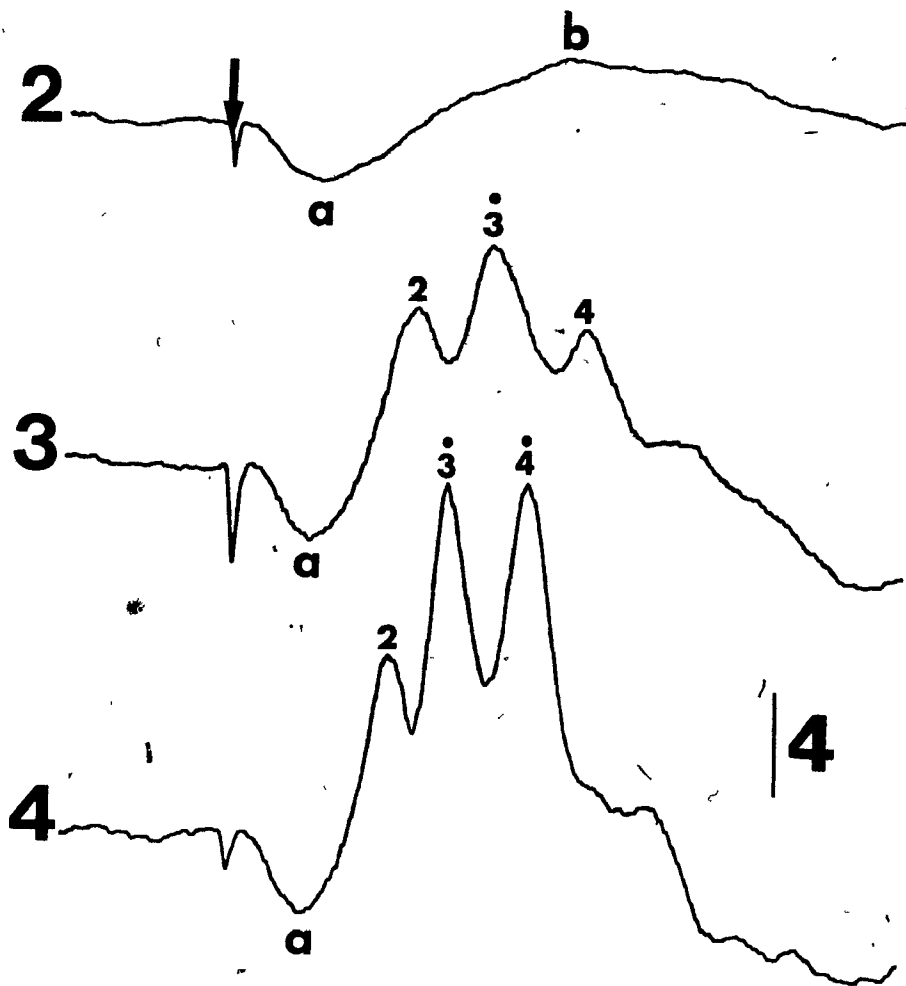


Figure 11: Maturation of the light-adapted ERG: weekly measurements (background: 520 lux; flash intensity: 10 cd/m²/sec)

The recording at week 4 presents a difficulty in determining the site of the b-wave, based on the definition of the latter as the most positive wave (see text). The vertical arrow indicates flash onset.

Calibration: horizontal bar in milliseconds, vertical bar in microvolts.

W
E
E
K



12

Discussion

Dark Adaptation

As shown in figure 5, the b-wave and OP peak times change simultaneously and the SOP/b-wave amplitude ratio is constant, as the rabbits age. This is in contrast to the results of Hamasaki and Maguire (1985) in the case of the kitten, where OPs developed at a slower rate than the b-wave. Sanada (1964b), however, noted the appearance of OPs in rabbits as early as that of the negative wave (a-wave), in concert with our results. The b-wave in the rabbit develops with increasing amplitude and decreasing peak time to age 40 days, as noted by Reuter (1976). We also note a progressive increase in amplitude and decrease in peak time of the b-wave and OPs with the bright flash.

The b-wave parameters change similarly when the dim flash is used. The OPs, however, are not visible until the fifth week (figure 7). This apparent inconsistency results from the effect of the recording filter, as shown in figure 8, where OPs are not demonstrated on the 100-1000 Hz recording but are seen on the 30-1000 Hz tracing. This is caused by attenuation of frequencies below 100Hz in the former case; the lower the frequency from 100 Hz, the greater the attenuation. The standard choice of a 100-1000 Hz bandwidth has been recommended for normal human OP recordings, where the OPs were shown to be in the 125

to 150 Hz range (Gur and Zeevi, 1980; McCulloch et al., 1972; Tsuchida et al., 1973). In the dark adapted rabbit, however, OPs evoked with a dim flash at week 5 are of a frequency domain closer to 90 Hz, resulting in a greater attenuation by the 100-1000 Hz bandwidth filter. The frequency domain of the OPs is not only dependent on the level of maturation reached by the retina, as shown in figure 5 (OP-OP interval), but on the intensity of the stimulus as well (dim versus bright light). The 100-1000 Hz filter is inappropriate in our setting, when the dim stimulus is used, and may be inappropriate for abnormal human recordings where OPs have been shown to be selectively abolished, as in diabetic retinopathy (Brunette and Desrochers, 1970; Speros and Price, 1981). Similarly, the results of Hamasaki and Maguire (1985) that cat OPs develop later than the b-wave, may have been caused by their choice of recording filter bandwidth (100-1000 Hz) to record the OPs. Sanada (1964) chose a 15 Hz low frequency cut-off to record data, with a different result for reasons as explained above.

Reuter (1976) described two b-wave processes in the growing rabbit, in dark adaptation: the "slow b-wave" of low threshold, long peak latency and no OPs, seen with low stimulus intensity; and the "fast b-wave" of higher threshold, shorter latency and presence of OPs, seen with high stimulus intensity. We find, however, that OPs are seen with the dim flash

when recorded with a 30-1000 Hz bandwidth. The OPs integrate to form a b-wave with a smooth appearance, but on closer inspection form irregularities on the rising slope of this wave (figure 8). These irregularities are also seen in Reuter's (1976) recordings. A change in frequency domain of the OPs with changing light intensity would explain his apparent two b-wave processes. The b-wave peak times appear to change irregularly within the second week (figure 6). However, the integration of OPs to form the ERG would explain this finding, as new OPs appear and contribute to the most positive portion of the ERG waveform. As seen in figure 6, OP2 is noted first, followed by the development of OP3 and OP4. A similar sequential formation of OPs in dark adaptation was also noted by others in rabbits (Sanada, 1964a, 1964b) and kittens (Hamasaki and Maguire, 1985). After week 2, however, all OPs are present with unchanging relative contributions, resulting in a regular and predictable change of b-wave parameters (amplitude and peak time) with age.

Light Adaptation

The photopic b-wave and OP amplitudes increase, and peak times decrease, with age. The measurement of some recordings, however, yields b-wave peak times that change irregularly with age, as in figure 10C, where the b-wave peak time decreases from the second to the fourth week but increases at the fifth week. The peak time of any individual wave in the recording decreases at a regular rate, from the time that it is clearly visible at week 3. However, the b-wave peak time changes depending on which individual wave has the highest amplitude. The b-wave peak time (figure 10C) can be seen to correspond to wave 3 at the fourth week, but to wave 4 at the fifth week. It is this shift that results in a sudden increase in b-wave peak time, a result which points to the arbitrary nature of the definition of the b-wave.

The recording at the fourth week in figure 11, where waves 3 and 4 are of equal height, presents a problem in identification of the peak of the b-wave. The view as established by Cobb and Morton (1954) would be of an OP (wave 3) superimposed on the b-wave (which corresponds to wave 4). The amplitude of wave 3 is at first higher than that of wave 4 at the third week, becoming equal in height at the fourth week. The view that wave 3 is an OP superimposed on the b-wave (wave 4), at the fourth week, requires that this also hold for the third week; this OP (wave 3) would be ?

larger than the b-wave (wave 4) at this stage, a view inconsistent with that of an ERG containing OPs that ride on the rising slope of the b-wave. The results are therefore more compatible with the view that waves 3 and 4 are building blocks of the ERG, corresponding to OP3 and OP4, respectively. The individual numbered waves of the ERG correspond to those on the 100-1000 Hz recording. The OPs are more visible on the 100-1000 Hz recordings, as they are higher frequency components which are selectively recorded by this bandwidth (Gur and Zeevi, 1980; McCulloch et al., 1972; Tsuchida et al., 1973).

The b-wave takes form with age, as the OPs develop in amplitude, decrease in peak time and increase in frequency domain from 99 ± 16 Hz at week 3, to 119 ± 10 Hz at week 5. The contribution of changing OP amplitudes and peak times, to b-wave genesis, has been described elsewhere (Lachapelle, 1985a, 1985b; Lachapelle et al, 1983, 1986a, 1986b). The b-wave peak time reflects the peak time of the OP that happens to contribute to the most positive portion of the b-wave at a specific age. Similarly, Berson et al. (1969) found that the addition of new OPs, with increasing light stimulus, "complicated" the measurement of the human photopic b-wave peak time because of their overriding the basic waveform. The peak time of the b-wave increased with an increase in flash intensity.

Conclusions

1. The a-wave is the first ERG wave to appear in a consistent way. It is recorded as soon as the eyes are open (day 7).
2. The b-wave and OP amplitudes and peak times change at the same rate (Figures 4,5,6,9,10). This is compatible with the view that OPs are major building blocks of the ERG.
3. The b-wave peak times change irregularly within the second week in dark adaptation (Figure 6) and, in some cases, in light adaptation (figures 10,11). The integration of OPs to form the ERG signal would explain this finding, as the ERG waveform correlates with the number of OPs, their relative amplitudes and frequency domains.
4. The maturation sequence is as follows : a-wave...OP2...OP3 & OP4.
5. The frequency domain of the OPs needs to be taken into consideration in choosing a recording bandwidth (figures 7,8).

The origin of the OPs appears to be stratified within the retina (Wachtmeister and Dowling, 1978) and there is evidence that they may originate from different retinal structures (Gutierrez and Spiguel, 1973; Heynen and van Norren, 1985; Wachtmeister and Dowling, 1978; Pacheco and Muzquiz, 1982). Our results show that the addition of these OPs directly predicts

the change in b-wave morphology with age. This suggests, contrary to previously published material, that the OPs are important contributors to b-wave genesis, since they are responsible for its peak time and amplitude.

The ERG is the only clinical test now available to permit an objective evaluation of the functional integrity of the retina. At present, clinical interpretation is restricted to the measurement of the amplitude and peak time of the b-wave. This study shows that the OPs are of major importance in forming the b-wave and should be regarded as primary visual events when examining ERG changes in disease. It is hoped that this will increase the diagnostic usefulness of the ERG.

Acknowledgements

I would like to thank Dr. Pierre Lachapelle for his teaching and support, the use of his laboratory and materials, and for reviewing the manuscript. I would also like to thank the McGill University-Montreal Children's Hospital Research Institute for the use of the facility and for financial assistance.

References

Bonaventure N, Goswamy S, Karli P (1967) Maturation des potentiels ERG et évoqués visuels chez le lapin-élevé dans des conditions naturelles d'éclairment ambiant. CR Soc Biol (Paris) 161:689-693

Brindley GS (1956) Responses to illumination recorded by microelectrodes from the frog's retina. J Physiol (Lond) 134:360

Brindley GS (1957) The passive electrical properties of the retina and the sources of the electroretinogram. Bibl Ophthalmol 48:24-31

Brown KT, Murakami M (1964) A new receptor potential of the monkey retina with no detectable latency. Nature Lond 201:626-628

Brown KT, Wiesel TN (1961) Analysis of the intraretinal electroretinogram in the intact cat eye. J Physiol Lond 158:229-256

Brown KT, Wiesel TN (1961) Localization of origins of electroretinogram components by intraretinal recording in the intact cat eye. J Physiol Lond 158:257-280

Brown PK, Wald G (1964) Visual pigments in single rods and cones of the human retina. Science 144:45

Brunette JR, Desrochers R (1970) Oscillatory potentials: a clinical study in diabetics. Can J

Ophthalmol 5:373-380

Burian HM, Allen LA (1954) A speculum contact lens electrode for electroretinography. Electroenceph Clin Neurophysiol 6:509-511

Cohen AI (1972) Rods and cones. In Fuortes Handbook of sensory physiology. Springer-Verlag, Berlin 7:2

Cobb WA, Morton HB (1954) A new component of the human electroretinogram. J Physiol 123:36-37

Dartnall HJ, Bowmaker JK, Mollon JD (1983) Human visual pigments: microspectrophotometric results from the eyes of seven persons. Proc Roy Soc (Lond) 220(B):115

Davis FA (1929) The anatomy and histology of the eye and orbit of the rabbit. Trans Am Ophthalmol Soc 27:401-441

Dawson WW, Stewart HL (1968) Signals within the electroretinogram Vision Res 8:1265-1270

Dowling JE (1970) Organization of vertebrate retinas. Invest Ophthalmol 9:655

Faber DS (1969) Analysis of the slow transretinal potentials in response to light. PhD dissertation State Univ NY at Buffalo

Fatechand R (1978) Rod and cone generation of wavelets in the frog electroretinogram. Vision Res 18:229-232

Granit R (1947) Sensory mechanisms of the retina.
Oxford Univ Press

Granit R (1962) The visual pathway. In *The Eye* 2:537-691

Gum GG, Gelatt KN, Samuelson DA (1984) Maturation of the retina of the canine neonate as determined by electroretinography and histology. *Am J Vet Res* 45(6):1166-1171

Gur M, Zeevi Y (1980) Frequency domain analysis of the human electroretinogram. *J Opt Soc Am* 70:53-59

Gutierrez C, Spiguel RD (1973) Oscillatory potentials of the cat retina. Effects of adrenergic drugs. *Life Sci* 13:991-999

Hagins WA, Penn RD, Yoshikami S (1970) Dark current and photocurrent in retinal rods. *Biophysiol J* 10:380-412

Hamasaki DI, Maguire GW (1985) Physiological development of the kitten's retina: an electroretinographic study. *Vision Res* 25(11):1537-1543

Henkes H (1951) Use of electroretinography in measuring the effects of vasodilatation. *Angiology* 2:125

Heynen H, van Norren D (1985) Origin of the electroretinogram in the intact macaque eye.II. Current

source density analysis. Vision Res 25:709-715

Hughes A (1971) Topographical relationships between the anatomy and physiology of the rabbit visual system. Doc Ophthalmol 30:33-159

Johnson MA, Massof RW (1982) The photomyoclonic reflex: an artefact in the clinical electroretinogram. Br J Ophthalmol 66:368-378

Karpe G (1945) The basis of clinical electroretinography. Acta Ophthalmol Suppl 24:1-118

Kozak WM (1971) Electroretinogram and spike activity in mammalian retina. Vision Res Suppl 3:129-149

Lachapelle P, Little JM, Polomeno RC (1983) The photopic electroretinogram in congenital stationary night blindness with myopia. Invest Ophthalmol Vis Sci 24:442-450

Lachapelle P (1985a) Impact of the recording bandwidth on the electroretinogram. Can J Ophthalmol 20(6):211-215

Lachapelle P (1985b) Oscillations on the electroretinogram: a synthetic approach. Can J Ophthalmol 20(6):216-219

Lachapelle P, Molotchnikoff S (1986a) Components of the electroretinogram: A reappraisal. Doc Ophthalmol 63:337-348

Lachapelle P, Molotchnikoff S (1986b) A composite nature for the photopic b-wave of the (human electroretinogram as evidenced by the use of the 60 Hz notch filter. Can J Ophthalmol 21(1):19-22

McCulloch C, Orpin JA, Waisberg JW et al (1972) Frequency analysis of the human dark adapted electroretinogram. Can J Ophthalmol 7:189-198

Miller RF (1973) Role of K⁺ in generation of the b-wave electroretinogram. J Neurophysiol 36:28-38

Miller RF, Dowling JE (1970) Intracellular response of the Müller (glial) cells of the mudpuppy retina. Their relation to the b-wave of the electroretinogram. J Neurophysiol 33:323-341

Nilsson SE, Knave B, Persson HE (1977) Change in ultrastructure and function of the sheep pigment epithelium and retina induced by sodium iodate II. Early effects. Acta Ophthalmol 55:1007-1026

Noell WK (1954) The origin of the electroretinogram. Am J Ophthalmol 38:78-90

Noell WK (1958) Studies on visual cell variability and differentiation. Ann NY Acad Sci 74:337-361

Nuboer JF, van Nuys WM, Wortel JF (1983) Cone systems in the rabbit retina revealed by ERG-null-detection. J Comp Physiol 151:347-352

Ogden T (1973) The oscillatory waves of the primate electroretinogram. Vision Res 13:1059

Ogden T, Wylie R (1971) Avian retina. I. Microelectrode depth and marking studies of local electroretinograms. J Neurophysiol 34:357

Pacheo P, Muzquiz L (1982) Two retinal processes displayed in the cat electroretinogram. Vis Res 22:1525-1532

Penn RD, Hagins WA (1972) Kinetics of the photocurrent of retinal rods. Biophysiol J 12:1073-1094

Reuter JH (1976) The development of the electroretinogram in normal and light deprived rabbits. Pflüger Arch 363:7-13

Rodieck RW (1973) The vertebrate retina principles of structure and function. W.H. Freeman and Company, San Francisco

Sanada T (1964a) Study on the electroretinogram on suckling rabbits. Report III. Studies on oscillatory small waves due to stimulation of white light. Nippon Ganka Gakkai Zasshi 68(12):1741-1746

Sanada T (1964b) Study on the electroretinogram on suckling rabbits. Report IV. Observation of oscillatory wavelets produced by monochromatic stimulation. Nippon Ganka Gakkai Zasshi 68(13):1859-1870

Speros P, Price J (1981) Oscillatory potentials. History, techniques and potential use in the evaluation of disturbances of retinal circulation. Surv Ophthalmol 25:237-252

Steinberg RH, Schmidt R, Brown KT (1970) Intracellular responses to light from cat pigment epithelium: origin of the electroretinogram c-wave. Nature (London) 227:728-730

Stodmeister R (1973) The spectral sensitivity functions of human ERG wavelets. Ophthalmol Res 5:21-30

Tomita T (1963) Electrical activity in the vertebrate retina. J Opt Soc Am 53:49-57

Tomita T (1970) Electrical activity of vertebrate photoreceptors. Q Rev Biophysiol 3:179-222

Tomita T (1976) Electrophysiological studies of retinal cell function. Invest Ophthalmol 15:171-187

Tomita T, Torihama Y (1956) Further study on the intraretinal action potentials on the site of ERG generation. Jap J Physiol 6:118-136

Tsuchida Y, Kawasaki K, Fujimura K, Jacobson JH (1973) Isolation of faster components in the electroretinogram and visually evoked response in man. Am J Ophthalmol 75:846-852

Wachtmeister L, Dowling JE (1978) The potentials of the mudpuppy retina. Invest Ophthalmol Vis Sci 17:1176-1188

Yonemura D, Aoki T, Tsuzuki K (1962) Electroretinogram in diabetic retinopathy. Arch Ophthalmol 68:19-24

Table 1A: Dark adapted data (flash intensity 3.2
cd/m²/sec)

The peak time (PT) is measured in milliseconds from flash onset. The amplitude (AMP) is measured in microvolts. The a-wave is a negative wave. The positive wave peaks are numbered; the highest one is the b-wave, by definition, and is underlined. OP parameters are measured on the 100-1000 Hz recordings, which includes those occurring, in time, up to the corresponding b-wave on the 1-1000 Hz recordings. Parameters that could not be measured, are marked with a dash.

(1-1000 Hz recording)

	a-wave		wave 1		wave 2		wave 3		wave 4	
	PT	AMP	PT	AMP	PT	AMP	PT	AMP	PT	AMP
Week 2	22.0	5.9								
	18.1	3.6	<u>27.0</u>	<u>3.6</u>	53.0	5.9				
	20.0	3.2	<u>32.0</u>	<u>3.8</u>						
	26.1	12.6	-	<u>4.2</u>						
	22.0	10.5								
Week 3	22.4	25.2	33.1	18.5	42.0	29.4	<u>55.2</u>	<u>45.9</u>		
	20.9	25.0	33.1	20.8	41.0	28.8	<u>53.6</u>	<u>38.4</u>	<u>60.1</u>	<u>41.1</u>
	20.4	39.7	29.6	24.6	37.8	40.5	<u>48.4</u>	<u>65.9</u>		
	22.8	18.9	33.7	19.5	<u>46.4</u>	<u>42.2</u>				
	20.0	32.6	28.4	22.1	35.8	35.5	<u>46.2</u>	<u>59.6</u>		
	18.2	27.1	25.9	16.8	33.8	35.9	<u>44.2</u>	<u>65.1</u>		
Week 4	17.2	38.9	25.0	31.5	31.9	62.0	<u>41.0</u>	<u>99.6</u>	62.0	55.2
	17.2	21.0	25.1	18.9	31.2	27.9	<u>41.8</u>	<u>50.8</u>	58.8	24.2
	14.8	16.2	24.1	10.9	30.8	18.5	<u>42.3</u>	<u>37.4</u>		
	17.4	14.3	34.0	35.1	<u>46.1</u>	<u>58.8</u>				
	18.0	19.9	27.0	19.9	32.6	35.5	<u>41.2</u>	<u>56.5</u>		
	16.2	31.7	24.3	25.0	30.0	52.9	<u>40.0</u>	<u>91.6</u>	48.1	57.5
Week 5	16.1	38.6	24.8	34.4	31.0	69.7	<u>38.9</u>	<u>109</u>	60.0	53.3
	16.2	33.6	24.8	24.2	30.0	42.0	<u>38.8</u>	<u>71.9</u>		
	15.4	32.3	23.2	19.3	29.4	38.0	<u>38.6</u>	<u>58.0</u>		
	16.8	24.8	24.5	25.8	31.8	42.0	<u>41.0</u>	<u>60.5</u>		
	15.8	21.8	25.1	22.9	30.0	43.4	<u>36.2</u>	<u>66.0</u>		
	15.4	10.1	23.8	14.3	29.7	23.5	<u>37.9</u>	<u>43.9</u>		

(100-1000 Hz recording)

	OP 2		OP 3		OP 4		OP 5	
	PT	AMP	PT	AMP	PT	AMP	PT	AMP
Week 2	-	-						
	22.4	0.4						
	25.0	0.5						
	34.0	1.2						
	23.9	1.2	36.1	0.6	48.0	0.6	70.0	0.7
Week 3	26.4	3.3	39.2	2.0	50.0	2.3		
	24.0	1.5	38.1	0.6	47.2	1.0	57.5	0.3
	26.1	5.0	35.6	3.1	45.2	6.3		
	-	-						
	22.1	4.5	33.8	3.4	42.0	7.1		
	22.5	4.2	31.0	4.7	40.4	8.6		
Week 4	20.5	7.3	29.2	3.6	38.8	6.8		
	20.0	3.8	30.1	2.2	38.8	5.6		
	20.4	4.0	29.2	2.5	40.2	5.5		
	-	-						
	21.8	4.1	30.8	1.9	37.8	4.6		
	20.0	6.2	27.9	5.0	36.4	10.0		
Week 5	17.0	7.3	25.9	4.0				
	21.2	5.8	28.1	2.2	37.2	7.4		
	18.3	6.0	25.8	2.9	35.2	5.4		
	20.8	4.8	29.6	4.3	39.1	6.7		
	19.5	4.6	27.8	2.7	34.2	6.3		
	19.2	2.7	27.8	2.1	34.6	5.9		

Interpeak interval average: week 3 10.3 ± 1.2 msec

week 5 8.2 ± 0.8 msec

(i.e., frequency domain increases with age from 97 Hz to 122 Hz)

Table 1B: Dark adapted data (flash intensity 0.32 cd/m²/sec).

In addition to 1-1000 Hz (ERG) recordings, 30-1000 Hz recordings were done at weeks 4 and 5 for which data are shown. The 100-1000 Hz recordings yielded poorly visible OPs which were not measurable.

(1-1000 Hz recording)

	a-wave		wave 1		wave 2		wave 3		wave 4	
	PT	AMP	PT	AMP	PT	AMP	PT	AMP	PT	AMP
Week 2	-	-								
	16.8	1.3	<u>28.0</u>	<u>1.8</u>	57.0	2.5				
	86.1	7.8								
	85.6	7.5								
Week 3	21.0	2.1	<u>78.0</u>	<u>12.2</u>						
	22.4	3.3	50.4	12.6	66.4	21.7	<u>81.6</u>	<u>22.5</u>		
	25.6	7.8	42.4	15.7	64.8	29.8	<u>77.6</u>	<u>31.3</u>		
	26.4	4.8	<u>83.2</u>	<u>19.2</u>						
	20.8	4.4	40.8	13.7	<u>72.0</u>	<u>31.2</u>				
	21.6	2.8	36.8	14.3	<u>58.4</u>	<u>32.5</u>				
Week 4	17.6	6.2	<u>59.2</u>	<u>65.8</u>						
	17.6	3.1	36.0	16.8	<u>57.1</u>	<u>27.3</u>				
	20.8	2.7	<u>54.4</u>	<u>17.7</u>						
	21.6	10.3	<u>59.2</u>	<u>40.3</u>						
	19.2	3.9	33.6	14.5	<u>57.6</u>	<u>30.2</u>				
	18.4	5.9	34.4	25.4	<u>51.2</u>	<u>50.6</u>				
Week 5	17.6	5.6	<u>50.4</u>	<u>71.7</u>						
	19.2	6.9	32.0	22.8	<u>56.8</u>	<u>46.2</u>				
	19.2	9.7	<u>47.2</u>	<u>45.0</u>						
	18.4	2.6	<u>52.8</u>	<u>38.5</u>						
	19.2	2.5	<u>55.2</u>	<u>39.6</u>						
	12.0	0.7	31.2	12.7	<u>56.8</u>	<u>26.5</u>				

(30-1000 Hz recording)

	OP 2		OP 3		OP 4		OP 5	
	PT	AMP	PT	AMP	PT	AMP	PT	AMP
Week 4	29.0	4.8	42.4	3.4				
Week 5	26.0	9.2	38.6	1.8				
	26.1	7.0	30.8	0.8	38.0	2.0	44.8	1.2
	26.0	7.4						
	29.4	6.0	37.9	1.6				
	25.8	5.2	40.0	2.0				
	30.1	4.4	41.5	3.4	58.0	2.0		

Interpeak intervals average to 11.1 ± 3.5 msec at week 5 (i.e. 90 Hz frequency domain)

Table 2: Light adapted data.

The peak time (PT) is measured in milliseconds from flash onset. The amplitude (AMP) is measured in microvolts. The a-wave is a negative wave. The positive wave peaks are numbered; the highest one is the b-wave, by definition, and is underlined. OP parameters are measured on the 100-1000 Hz recordings, which includes those occurring, in time, up to the corresponding b-wave on the 1-1000 Hz recordings. Parameters that could not be measured, are marked with a dash.

(1-1000 Hz recording)

	a-wave		wave 1		wave 2		wave 3		wave 4	
	PT	AMP	PT	AMP	PT	AMP	PT	AMP	PT	AMP
Week 2	22.0	2.7	<u>38.0</u>	<u>4.5</u>						
	13.6	4.0								
	18.4	2.1	<u>37.6</u>	<u>4.7</u>						
	27.2	8.7	<u>93.2</u>	<u>14.7</u>						
	11.6	7.1	<u>41.6</u>	<u>15.0</u>						
Week 3	12.0	9.1	25.6	30.0	<u>33.6</u>	<u>32.8</u>	43.2	25.7		
	10.4	8.8	24.8	29.3	<u>31.2</u>	<u>33.0</u>	54.4	13.0		
	12.0	11.6	25.6	33.4	<u>32.8</u>	<u>36.4</u>	39.2	32.4	55.2	12.1
	13.6	7.9	28.8	29.1	<u>38.4</u>	<u>33.6</u>				
	11.2	9.6	<u>23.2</u>	<u>41.2</u>						
	10.4	9.1	23.2	28.3	<u>32.0</u>	<u>42.3</u>	44.0	25.7	55.2	12.2
Week 4	9.6	11.6	20.8	35.7	<u>30.4</u>	<u>62.9</u>	36.0	44.7		
	10.4	6.2	21.6	24.9	<u>29.6</u>	<u>39.7</u>	38.4	24.8	48.8	13.9
	11.2	9.2	21.6	21.4	<u>28.8</u>	<u>38.2</u>	36.8	21.5		
	11.2	7.4	21.6	21.1	<u>30.4</u>	<u>36.3</u>	37.6	20.0	48.0	8.1
	11.2	10.7	20.8	28.8	<u>28.0</u>	<u>53.1</u>	35.2	40.1	44.1	19.4
	9.6	10.1	20.0	31.3	<u>27.2</u>	<u>62.7</u>	<u>36.8</u>	<u>62.7</u>	51.9	13.0
Week 5	8.8	10.0	19.2	43.1	<u>26.2</u>	<u>82.6</u>	34.4	53.4	47.2	15.7
	11.2	5.4	19.2	21.3	<u>27.2</u>	<u>40.7</u>	33.6	19.0	41.6	7.7
	11.2	7.6	20.8	30.8	<u>28.8</u>	<u>53.4</u>	36.0	26.7		
	10.4	8.4	20.8	28.8	<u>28.8</u>	<u>50.0</u>	36.0	29.4	47.2	11.4
	12.0	13.4	20.0	29.9	27.2	56.6	<u>34.4</u>	<u>82.7</u>	48.1	20.2
	9.6	8.0	19.2	29.7	<u>26.4</u>	<u>64.7</u>	40.8	14.8		

(100-1000 Hz recording)

	OP 2		OP 3		OP 4		OP 5	
	PT	AMP	PT	AMP	PT	AMP	PT	AMP
Week 2	-	-						
	19.5	1.2						
	20.0	7.0						
	16.9	1.8						
	14.2	1.5						
Week 3	20.6	3.6	31.6	1.7	41.2	1.6		
	20.0	3.9	29.0	1.1				
	20.5	4.0	31.4	2.2	37.1	1.2		
	-	-						
	18.0	4.3	30.6	4.5				
	18.4	3.7	29.6	5.8	41.0	4.5		
Week 4	16.4	6.5	25.8	9.8	35.4	3.6		
	16.9	3.5	27.1	6.1	36.6	3.8		
	18.2	3.4	28.1	6.5	37.2	4.8		
	17.2	3.4	27.0	5.9	35.9	2.6		
	18.1	6.2	26.2	9.4	33.6	7.3		
	17.5	5.6	25.0	12.0	34.1	12.8		
Week 5	15.5	7.8	23.5	15.9	31.7	9.4		
	15.6	4.5	24.5	6.6				
	16.2	5.8	25.4	9.7	34.2	4.5		
	16.4	4.8	25.2	9.9	33.0	4.1		
	19.0	7.6	26.4	8.6	33.8	9.5		
	16.2	4.6	24.4	11.6				

Interpeak interval average: week 3 10.1 ± 1.7 msec

week 5 8.4 ± 0.7 msec

(i.e. frequency domain increases with age from 99 Hz to 119 Hz)